PHYSICAL REVIEW B **88**, 060407(R) (2013)

Ferromagnetism with $T_C = 200$ K in the amorphous $5f$ compound $UH_3Mo_{0.18}$

I. Tkach,[1] S. Mašková,[1] Z. Matěj,[1] N.-T. H. Kim-Ngan,[2] A. V. Andreev,[3] and L. Havela[1]

[1]*Department of Condensed Matter Physics, Faculty of Mathematics and Physics, Charles University, Ke Karlovu 5, 12116 Prague 2, Czech Republic*

[2]*Institute of Physics, Pedagogical University, Podchorazych 2, 30-084 Krakow, Poland*

[3]*Institute of Physics, Academy of Sciences, Na Slovance 2, 18221 Prague, Czech Republic*

(Received 23 April 2013; revised manuscript received 27 June 2013; published 20 August 2013)

$UMo_{0.18}$ can absorb hydrogen at elevated H_2 pressures. The product is a compact but brittle hydride $UH_3Mo_{0.18}$, which is to some extent analogous to β-UH_3, but it is almost amorphous (the grain size smaller than 1.2 nm). It is ferromagnetic, and its Curie temperature (200 K) is higher, despite the disorder, than that of β-UH_3 ($\approx$170 K). We also registered an increase in U magnetic moments. The randomness, together with the large anisotropy inherent to U systems, leads to a very high coercivity, reaching 3.7 T at low temperatures. As amorphization normally tends to suppress magnetic ordering of U compounds, the hydride represents a different class of materials, amorphous U-based ferromagnets with relatively very high Curie temperatures.

DOI: 10.1103/PhysRevB.88.060407 PACS number(s): 75.50.Kj, 75.50.Vv, 72.15.Cz

Hydrogenation of uranium metal under normal conditions usually leads to β-UH_3 with a cubic structure ($Pm3n$ space group) and unit cell ($a \approx 6.64$ Å) containing eight U atoms.[1] The reaction is already observed at low H pressures, and it is one of the major concerns considering aging/degradation of U metal products. The very fine β-UH_3 powder also easily ignites at room temperature in air. Besides the high reactivity it is also the relatively low equilibrium H pressure (heating to almost 450 °C is necessary to reach the equilibrium pressure of 1 bar)[1] which prevents considering the relatively inexpensive U metal as a hydrogen storage medium.

An important aspect of β-UH_3 is its magnetic order already reported in 1952.[2] The crystal structure expanded by H (the shortest U-U spacing in β-UH_3 is 3.31 Å, in α-U it is merely 2.76 Å) leads to the formation of U magnetic moments of about $0.9\mu_B$/U, possibly the same for each of two different U positions. They order ferromagnetically with the Curie temperature of approximately 170 K,[1,3] which is in striking contrast to the weak Pauli paramagnetism of α-U.

The main reason for magnetic order is probably a reduction in the overlap of the $5f$ wave functions between nearest U neighbors, reducing the $5f$ bandwidth and increasing the density of states at the Fermi level $N(E_F)$. The Sommerfeld coefficient of the electronic specific heat γ indeed increases by more than a factor of 3 from α-U to β-UH_3 ($\gamma = 33.9$ mJ mol^{-1} K^{-2}).[4] The dramatic modification of the $5f$ states is actually demonstrated by high-resolution photoelectron spectroscopy.[5] A similar tendency to strengthen magnetic properties due to H-induced lattice expansion has been observed in numerous U-based intermetallic compounds.[6]

Applications of uranium as low-enriched nuclear fuel brought into focus the bcc form of U. It exists as the high-temperature phase of pure U metal (γ-U stable in the range of 1049–1408 K) (Ref. 1) and can be stabilized to a lower temperature by doping. Combining the Mo doping with ultrafast cooling, we have shown[7,8] that the splat-cooling method entirely suppresses the α-U phase for Mo concentration higher than 11 at. %. Long-term stability of such alloys at room temperature is excellent, and the persisting metallic luster suggests a good corrosion resistance. It is, therefore, very interesting to inspect whether such "stainless" uranium is also more resistant to hydrogen absorption. In the present Rapid Communication, we concentrate on interaction with hydrogen of the splat sample produced from the alloy U-15 at. % Mo, i.e., $U_{0.85}Mo_{0.15}$ or $UMo_{0.18}$, which is safely within the range of the bcc phase.

The hydrogenation experiments were undertaken with the $UMo_{0.18}$ splats, the preparation of which was described in Ref. 7. Their analysis by x-ray diffraction (XRD) and electron microscopy proved the single phase character with the proper bcc structure and lattice parameter $a = 3.44$ Å. A certain amount of UO_2 and UC was detected at the surface of the splat.

For the H absorption study, the splat was inserted into a reactor, which was then pumped down to $p = 2 \times 10^{-6}$ mbar and, subsequently, was filled by pure H_2 gas ($p = 800$ mbar). In this case, no H absorption was detected even after 100 h.

Next, we applied enhanced pressure (80 bar) of H_2 on the splat of the same composition $UMo_{0.18}$. Opening the reactor after 24 h revealed that the splat material was broken into 1–5-mm-long brittle dark lamellas, which indicated that some H-induced process took place. The material was then crushed and was subjected to an x-ray powder diffraction study, which indeed indicated structure changes, mainly characterized as amorphization (see below). We have to stress that, unlike the fine powder of β-UH_3, the hydride obtained is not pyrophoric, and its handling, including crushing, is safe. To quantify the amount of absorbed hydrogen, the $UMo_{0.18}$ hydride was decomposed in a close evacuated volume by heating to 500 °C. The total amount of the 3.0 H/U atom was obtained. Therefore, we denote the hydride as $UH_3Mo_{0.18}$. This finding indicates that the hydride is analogous to β-UH_3 despite its amorphous structure.

Sample characterization was performed by using a Bruker D8 advanced diffractometer with Cu $K\alpha$ radiation. Figure 1 reveals several broad peaks, which can be attributed to diffraction lines of β-UH_3 subjected to a severe broadening. A quantitative analysis shows that the experimental pattern can be well reproduced assuming the broadening due to very small grains, the size of which is between nanocrystalline and amorphous structures. The size distribution has to be simulated

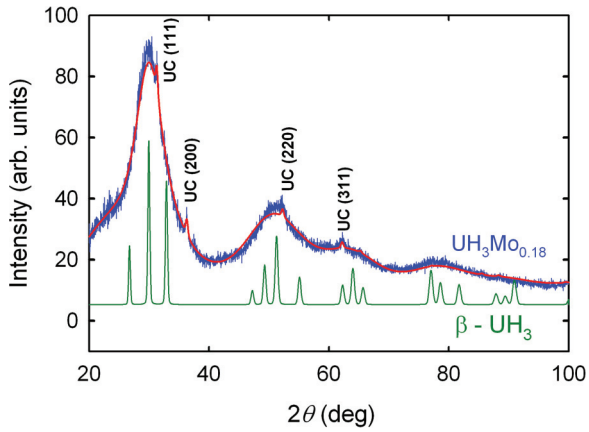

FIG. 1. (Color online) XRD pattern (Cu $K\alpha$ radiation) of $UH_3Mo_{0.18}$ (blue) compared with the simulated XRD pattern of β-UH_3 (green) and our fit of the experimental data fitting (red), which was used for the grain-size calculation.

using the Rafaja model[9] assuming grains of two different sizes, namely, 7 and 12 Å. The lattice parameter received, $a = 6.67$ Å is not far from value observed on β-UH_3 ($a = 6.64$ Å).

The material obtained was subjected to magnetization measurements in the temperature range of 2–300 K and in magnetic fields up to 14 T using the Quantum Design physical property measurement system equipment. One of the lamellas was used to measure the temperature dependence of electrical resistivity using four silver-pasted contacts and current along the lamella long axis. Specific heat was measured in the temperature range of 2–300 K on a pellet made of crushed and pressed material.

The temperature dependence of electrical resistivity, shown in Fig. 2, exhibits a dominant weak negative slope ($d\rho/dT < 0$) throughout the whole temperature range. Such a negative slope already was detected for the U-Mo alloys with the bcc structure.[10] Its reason can be seen in weak localization,[11] which appears under conditions of strong disorder and which is partly suppressed by electron-phonon scattering. It is nowadays believed to give an explanation for the Mooij criterion, relating the appearance of the negative slope to enhanced residual resistivity ρ_0.[12] The additional disorder introduced by amorphization cannot contribute much, the slope remains negative, but a pronounced kink appears at $T = 200$ K, undoubtedly related to magnetic ordering (Curie temperature, as seen below). Such a value is approximately 25 K higher than literature data for β-UH_3. The absolute resistivity values are unusually high, exceeding 1000 $\mu\Omega$ cm. The resistivity, which was studied for UD_3, also reaches similar values (over 600 $\mu\Omega$ cm).[4] An explanation for the very high resistivity values can be seen in the reduction in concentration of conduction electrons due to H absorption.

The temperature dependence of magnetization measured in various magnetic fields indicates ferromagnetic ordering with T_C close to 200 K. Although the paramagnetic range covered is short, it does allow for extracting a reliable value of the effective paramagnetic moment $\mu_{\text{eff}} = 2.40\mu_B$/U, which is in line with the data given for β-UH_3 or UD_3 (Ref. 1). The paramagnetic Curie temperature $\theta_p = 205$ K is 25–40 K higher than the values given for β-UH_3 or UD_3.[1]

Figure 3 displays hysteresis loops at selected temperatures. With the temperature decreasing down to 5 K, the coercive field strongly increases and reaches its maximum value ≈3.5 T. At $T = 1.7$ K, the character of the hysteresis loop changes. An abrupt Barkhausen-type reproducible jump appears between 3.6 and 3.7 T, which is followed by another more smooth increase in still higher fields. Such a behavior can be tentatively associated with the pinning of domain walls in highly disordered systems with high anisotropy. There exists extended evidence of similar behavior among such materials, labeled as high anisotropy random distribution, for example, on the basis of $SmCo_5$.[13] The magnetization behavior in still higher fields is almost reversible, which means that there is either additional rotation towards the field direction or there is a pronounced development of the size of magnetic moments (suppression of longitudinal spin fluctuations) or both effects. Comparing with the high-field susceptibility of β-UH_3, which is non-negligible but is smaller than for $UH_3Mo_{0.18}$, we can assume that both effects coexist in high magnetic fields. The high magnetic

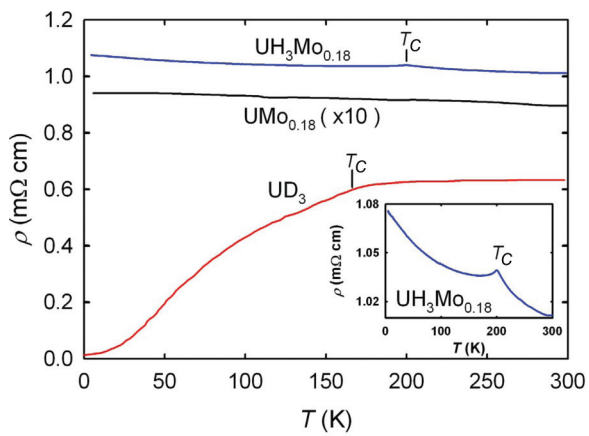

FIG. 2. (Color online) Temperature dependence of electrical resistivity of $UH_3Mo_{0.18}$ compared with the $UMo_{0.18}$ alloy and the data for UD_3 (analogy to β-UH_3) taken from Ref. 4. The inset shows the kink at $T = 200$ K correlating with T_C.

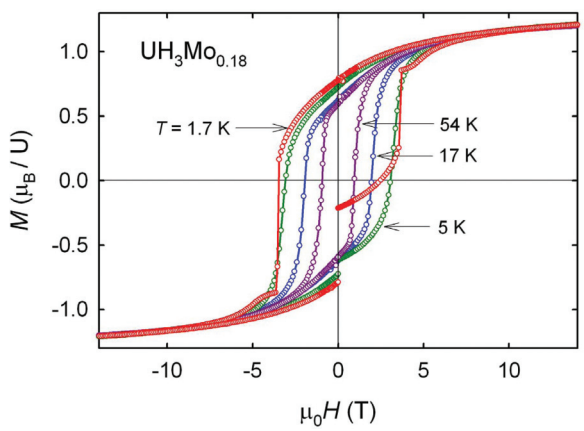

FIG. 3. (Color online) Field dependence of magnetization of $UH_3Mo_{0.18}$ measured at various temperatures. The negative magnetization at which the virgin curve starts could have been imposed by cooling in the weak residual negative field of the superconducting coil.

anisotropy itself is not exceptional among U compounds. It is due to large orbital moments (due to strong spin-orbit interaction) even in itinerant magnets and involvement of the $5f$-$5f$ bonding between nearest neighbors.[14]

Comparing to the size of spontaneous magnetization of β-UH_3 [$0.87\mu_B$/U at 4 K (Ref. 3)], $UH_3Mo_{0.18}$ has the values undoubtedly higher. However, it is not easy to determine a more exact value. The high anisotropy randomly distributed almost on the atomic scale effectively leads to a noncollinear ferromagnetism. Aligning the moments by the brute force of the high external magnetic field presumably leads to the enhancement of the size of moments by the field. Nevertheless, we can make a rough estimate of the spontaneous magnetization as corresponding to $\mu_U \approx 1.0\mu_B$ for $UH_3Mo_{0.18}$.

From the field dependence (up to 14 T) at $T = 1.7$ K, an estimate of the saturated moment can be performed assuming a phenomenological relation $M(H) = M_s[1 - a/H^2] + \chi_{hf}H$ where the second term accounts for the influence of field on the size of individual moments, whereas the first accounts for the anisotropy. The value obtained, $M_s = 1.15\mu_B$/U, is still far below the ionic moments ($\approx 3.2\mu_B$ for f^2 or f^3), which is in line with the strongly itinerant magnetism of the U hydrides. One can compare with literature data on β-UH_3, exhibiting a linear dependence of magnetization in fields. The high-field measurement[3] gives the slope of magnetization $\chi_{hf} = 0.0028\mu_B$/T) for β-UH_3. Fitting the data on $UH_3Mo_{0.18}$ to the formula above yields $0.005\mu_B$/T, corresponding to 3.8×10^{-8} m^3/mol.

For a more accurate determination of the Curie temperature we also measured the field dependences of magnetization at various temperatures from 170 to 200 K for the Arrott plot analysis. As conventional Arrott plots are often curvilinear at such temperatures due to critical phenomena, we used the modified Arrott plots procedure $M^{2.22}$ vs $(\mu_0 H/M)^{0.79}$,[15] which gives a more linear dependence. For comparison, we also used the same procedure for the data of β-UH_3. This method gave $T_C = 197.3$ K for $UH_3Mo_{0.18}$, which is about 30 K higher than for β-UH_3.

The temperature dependence of the specific heat of $UH_3Mo_{0.18}$ in comparison with the literature data of β-UH_3 (Ref. 16) is presented in Fig. 4. It displays the anomaly related to the Curie temperature of $UH_3Mo_{0.18}$ shifted to higher temperatures (near 200 K). Comparing to the data of β-UH_3, the transition is visibly broadened. That may indicate certain T_C distribution between grains due to disorder in the sample. One can also expect a difference in critical behavior in a system with a high anisotropy of a random type.

The low-temperature part can be approximated by the Debye model from which it is possible to estimate the Sommerfeld coefficient of the electronic specific heat. A linear fit (Fig. 4 inset) of C_P/T vs T^2 can be used in the temperature range below 50 K^2, which yields the value of $\gamma = 27.6$ mJ mol^{-1} K^{-2}. However, the best fit (Fig. 4 inset, red line) was obtained with an additional contribution to specific heat $C = \gamma T + \beta T^3 + \alpha T^{1/2}\exp(-T_0/T)$ where the last term accounts for magnons with the gap energy $k_B T_0$, which is the measure for the magnetic anisotropy energy per one U ion. This fit yields $\gamma = 29.2$ mJ mol^{-1} K^{-2} and $T_0 = 36$ K. This value is in good agreement with part of literature data

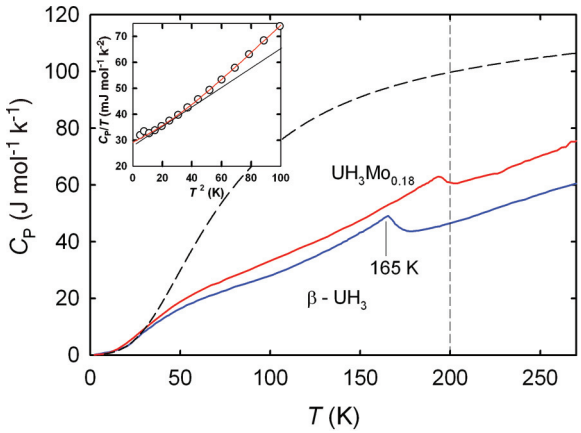

FIG. 4. (Color online) Temperature dependence of specific heat of $UH_3Mo_{0.18}$ compared with the data on β-UH_3 (from Ref. 16). The dashed curve corresponds to the Debye model (see the text) plus the linear contribution of the electronic specific heat. Inset: low-temperature part of the C_P/T vs T^2 dependence with the linear fit (gray line) and the fit including a magnon term (red).

for β-UH_3 (29 mJ mol^{-1} K^{-2}—see Ref. 17) but is slightly lower than in Ref. 4 (33.9 mJ mol^{-1} K^{-2}). It is approximately three times higher than for α-U and 1.5 times higher than for γ-U (splat sample $U_{0.85}Mo_{0.15}$ has $\gamma = 16.0$ mJ mol^{-1} K^{-2},[7] which corresponds to 18.8 mJ mol^{-1} K^{-2} using the formula $UMo_{0.18}$). The value $T_0 = 36$ K represents the gap in the magnon spectrum due to magnetic anisotropy.

The increase in γ with respect to $UMo_{0.18}$ indicates an increase in $N(E_F)$, which can be attributed to the enhancement of the U-U spacing in the narrow $5f$ band situation. Such a fit also yields the estimated Debye temperature $\theta_D = 296$ K in $UH_3Mo_{0.18}$, which is slightly higher than that given in Ref. 17 for β-UH_3 (270 K) but is lower than in Ref. 4 (338 K). Using this value for the Debye function (with the addition of electronic contribution), we calculated the theoretical temperature dependence of specific heat (Fig. 4, dashed curve) based on the Debye model, assuming all 4.18 atoms contributing by acoustic modes. The fact that this model goes much higher than the real data can be understood by Einstein modes, some of them with high characteristic energy, better describing the H vibrations. Relatively high slope at room temperature indicates that the classical limit (104.26 J mol^{-1} K^{-1}) plus the electronic term (8.76 J mol^{-1} K^{-1} at 300 K) would be gradually approached at elevated temperatures.

Hydrogenation of several U-rich compounds has been described in literature. For instance, U_6Co, which is a weak paramagnet and superconductor, crystallizing in the body-centered tetragonal structure, quite remarkably forms the hydride U_6CoH_{18} with a structure almost identical (as well as the value of lattice parameter) to that of β-UH_3. U_6CoH_{18} is a ferromagnet with $T_C = 185$,[18] which is marginally higher than β-UH_3 ($\approx$170 K) (Ref. 3). A similar result is observed in U_6Fe, found to absorb H up to the stoichiometry U_6FeH_{17}. The Curie temperature reported ($T_C = 173$ K) is identical to that of β-UH_3.[19] U_6Mn and U_6Ni most likely behave in the same way.[20] Here, we notice that none of these hydrides is amorphous. Besides, the structure pattern of β-UH_3 dominates in all hydrides of these U-based compounds. On the basis of

^{57}Fe Mössbauer spectroscopy, it was suggested that Fe atoms occupy one of the two U positions of the β-UH_3 structure.[19] In the case of the hydride of the splat-cooled U-Mo alloys exhibiting the bcc phase, such as $UH_3Mo_{0.18}$, the amorphization induced by hydrogenation was obtained. We have to point out here that the amorphization due to hydrogenation is not uncommon. It was already found, for example, in numerous rare-earth Laves phases[21–23] or compounds, such as La_2Pd_2In,[24] especially when hydrogenation was performed without increasing temperature. The reason can be seen in the tendency to locally form a structure pattern which does not allow a periodic coverage of a three-dimensional lattice. We may speculate that the reason for the amorphization is that Mo, unlike Fe, is not able to substitute U in the regular β-UH_3 lattice. Lack of affinity of Mo to H, which does not form any binary hydride, certainly plays a role because Mo with its atomic radius 1.40 Å is closer to U (1.56 Å) than Fe (1.26 Å), so the Mo substitution would be easier, seen from the point of view of atomic size. A model assuming that we deal with regular β-UH_3 with the coherence disrupted by Mo atoms with the mean spacing below 10 Å can explain the 1U-3H ratio maintained in the hydride.

As to magnetism, we cannot expect any contribution from Mo with a rather broad 4*d* band. The fact that we obtained an amorphous compound with 5*f* ferromagnetism at 200 K is quite extraordinary. Rapid quenching techniques succeeded to amorphize some U alloys, such as $U_{66}T_{34}$ (T = Fe,Co,Ni), which were reported to exhibit spin-glass characters and very low magnetizations.[25] In fact, such metallic glasses were later found to be superconducting.[26] Ternary amorphous (and icosahedral) materials of the type $Pd_{60}U_{20}Si_{20}$ were also found to be nonmagnetic, resembling to some extent UPd_3.[27] Early attempts to synthesize amorphous materials by sputter deposition were performed without dedicated UHV equipment and most likely led to the production of amorphous oxidic materials.[28] Nanocrystalline UFe_{2+x}'s have T_C exceeding 200 K, but the magnetic ordering is driven mostly by the Fe-3*d* magnetism.[29] The same situation is very probable for sputter-deposited films of such composition.[30] In fact, experiments with introducing disorder in a gradual way into the antiferromagnet UN (Ref. 31) or ferromagnet US (Ref. 32) indicate a tendency to suppress magnetic ordering and the size of magnetic moments. In this context, the enhancement of the Curie temperature in amorphous material comparing to β-UH_3 is very surprising. We assume that the commonly seen suppression of U magnetism due to randomization can be due to the sign of exchange interactions, varying from one site to another, amounting eventually to the moment destruction in the band magnetic systems. On the other hand, β-UH_3 can still be in the range of purely ferromagnetic interaction between nearest neighbors, so the variation in the U-U spacings does not act destructively. Supporting arguments are both theoretical works on hybridization-induced exchange interactions, which is ferromagnetic in the short U-U (bonding) directions,[33] and systematic occurrence of 5*f* ferromagnetism only at moderate U-U spacings, whereas, at high spacings antiferromagnetism dominates.[34] The increase in T_C could be attributed to somewhat higher 5*f* localization due to increasing mean U-U spacing (due to embedded Mo atoms), as opposed to the negative effect of hydrostatic pressure on β-UH_3.[3] The reasons for the T_C variations can be, however, less explicit, as shown by the theoretical analysis of the T_C enhancement due to amorphization in Co as opposed to Fe.[35] Experiments with varying concentrations of Mo or other dopants as well as experiments under pressure should bring more light to this issue.

This work was supported by the Czech Science Foundation under Grant No. P204/12/0285. I.T. was supported by the Grant Agency of the Charles University under Project No. 675112. Experiments were partly performed at MLTL (http://mltl.eu/), which is supported within the program of Czech Research Infrastructures (Project No. LM2011025).

[1] I. Grenthe, J. Drozdynski, T. Fujino, E. C. Buck, T. E. Albrecht-Schmitt, and S. J. Wolf, in *Chemistry of the Actinide and Transactinide Elements*, edited by L. R. Morss, N. M. Edelstein, and J. Fuger (Springer, The Netherlands, 2006), Vol. 1, p. 253.

[2] W. Trzebiatowski, A. Sliwa, and B. Stalinski, Roczn. Chem. **26**, 110 (1952).

[3] A. V. Andreev, S. M. Zadvorkin, M. I. Bartashevich, T. Goto, J. Kamarad, Z. Arnold, and H. Drulis, J. Alloys Compd. **267**, 32 (1998).

[4] J. W. Ward, L. E. Cox, J. L. Smith, G. R. Stewart, and J. H. Wood, J. Phys. (Paris) **40**, C4–15 (1979).

[5] T. Gouder, A. Seibert, J. Rebizant, F. Huber, and L. Havela, *Comparative Photoemission Study of Actinide (Am, Pu, Np and U) Metals, Nitrides, and Hydrides*, MRS Symposia Proceedings, Vol. 986, edited by K. J. M. Blobaum, E. A. Chandler, L. Havela *et al.* (Materials Research Society, Warrendale, PA, 2007), pp. 17–28.

[6] L. Havela, K. Miliyanchuk, and A. Kolomiets, Int. J. Mater. Res. **100**, 1182 (2009).

[7] I. Tkach, N.-T. H. Kim-Ngan, S. Mašková, M. Dzevenko, and L. Havela, J. Alloys Compd. **534**, 101 (2012).

[8] N.-T. H. Kim-Ngan, I. Tkach, S. Maškova, A. P. Goncalves, and L. Havela, J. Alloys Compd. **580**, 223 (2013).

[9] D. Rafaja, V. Klemm, G. Schreiber, M. Knapp, and R. Kuzel, J. Appl. Crystallogr. **37**, 613 (2004).

[10] B. S. Chandrasekhar and J. K. Hulm, J. Phys. Chem. Solids **7**, 259 (1958).

[11] Y. Imry, *Introduction to Mesoscopic Physics* (Oxford University Press, Oxford, 2002).

[12] J. H. Mooij, Phys. Status Solidi A **17**, 521 (1973).

[13] H. Oesterreicher, F. T. Parker, and M. Misroch, J. Magn. Magn. Mater. **15–18**, 1485 (1980).

[14] S. Mašková, A. M. Adamska, L. Havela, N.-T. H. Kim-Ngan, J. Przewoźnik, S. Daniš, K. Kothapalli, A. V. Kolomiets, S. Heathman, H. Nakotte, and H. Bordallo, J. Alloys Compd. **522**, 130 (2012).

[15] P. H. Frings, J. J. M. Franse, and P. E. Brommer, J. Phys. C **18**, 1955 (1985).

[16]R. Troc and W. Suski, J. Alloys Compd. **219**, 1 (1995).
[17]J. C. Fernandes, M. A. Continentino, and A. P. Guimaraes, Solid State Commun. **55**, 1011 (1985).
[18]A. V. Andreev, M. I. Bartashevich, A. V. Deryagin, L. Havela, and V. Sechovský, Phys. Status Solidi A **98**, K47 (1986).
[19]H. Drulis, F. G. Vagizov, M. Drulis, and T. Mydlarz, Phys. Rev. B **52**, 9500 (1995).
[20]H. Ito, K. Yamaguchi, T. Yamamoto, and M. Yamawaki, J. Alloys Compd. **271–273**, 629 (1998).
[21]K. Aoki, T. Yamamoto, and T. Masumoto, Scr. Metall. **21**, 27 (1987).
[22]A. V. Deryagin, A. A. Kazakov, N. V. Kudrevatykh, V. N. Moskalev, N. V. Mushnikov, and S. V. Terent'yev, Fiz. Met. Metalloved. **60**, 295 (1985) [Phys. Met. Metallogr. **60**(2), 81 (1985)].
[23]K. H. J. Buschow, Physica B **86–88**, 79 (1977).
[24]A. V. Kolomiets, S. Mašková, L. Havela, Z. Matěj, and R. Kužel, J. Alloys Compd. **501**, 4185 (2011).
[25]S. G. Cornelison, G. Hadjipananyis, and D. J. Sellmyer, J. Non-Cryst. Solids **40**, 429 (1980).
[26]M. Robrecht, J. Hasse, E.-W. Scheidt, and K. Lüders, Z. Phys. B **85**, 249 (1991).
[27]S. J. Poon, A. J. Drehman, and K. R. Lawless, Phys. Rev. Lett. **55**, 2324 (1985).
[28]P. Fumagalli, T. S. Plaskett, D. Weller, T. R. McGuire, and R. J. Gambino, Phys. Rev. Lett. **70**, 230 (1993).
[29]L. Havela, K. Miliyanchuk, A. P. Gonçalves, J. C. Waerenborgh, L. C. J. Pereira, P. Gaczynski, E. B. Lopes, and J. Pesicka, Intermetallics **19**, 113 (2011).
[30]N.-T. H. Kim-Ngan, L. Havela, A. M. Adamska, S. Daniš, J. Pešička, J. Macl, R. Eloirdi, F. Huber, T. Gouder, and A. G. Balogh, J. Phys.: Conf. Ser. **303**, 012012 (2011).
[31]D. Rafaja, L. Havela, R. Kuzel, F. Wastin, E. Colineau, and T. Gouder, J. Alloys Compd. **386**, 87 (2005).
[32]L. Havela, K. Miliyanchuk, D. Rafaja, T. Gouder, and F. Wastin, J. Alloys Compd. **408–412**, 1320 (2006).
[33]B. R. Cooper, R. Siemann, D. Yang, P. Thayamballi, and A. Banerjea, in *Handbook on the Physics and Chemistry of the Actinides*, edited by A. J. Freeman and G. H. Lander (North-Holland, Amsterdam, 1985), Vol. 2, p. 435.
[34]V. Sechovský and L. Havela, in *Ferromagnetic Materials*, edited by E. P. Wohlfarth and K. H. J. Buschow (North-Holland, Amsterdam, 1988), Vol. 4, p. 309.
[35]R. F. Sabiryanov, S. K. Bose, and O. N. Mryasov, Phys. Rev. B **51**, 8958 (1995).